NIH Public Access
Author Manuscript
Acta Biomater. Author manuscript; available in PMC 2014 November 01.

Published in final edited form as:
Acta Biomater. 2013 November ; 9(11): 8802–8814. doi:10.1016/j.actbio.2013.06.021.

Thiol-ene Michael-type formation of gelatin/poly(ethylene glycol) biomatrices for three-dimensional mesenchymal stromal/stem cell administration to cutaneous wounds

Kedi Xu[a,b,1], **David Antonio Cantu**[a,c,1], **Yao Fu**[a], **Jaehyup Kim**[d], **Xiaoxiang Zheng**[b], **Peiman Hematti**[e,f], and **W. John Kao**[a,c,f,g,*]

[a]School of Pharmacy, Division of Pharmaceutical Sciences, University of Wisconsin-Madison, 777 Highland Avenue, Madison, WI 53705, USA

[b]Quishi Academy for Advanced Studies, Zhejiang University, Hangzhou 310027, PR China

[c]Department of Biomedical Engineering, College of Engineering, University of Wisconsin-Madison, Madison, WI 53705, USA

[d]Department of Cellular and Molecular Biology, University of Wisconsin-Madison, Madison, WI 53705, USA

[e]Department of Medicine, Division of Hematology/Oncology, School of Medicine and Public Health, University of Wisconsin-Madison, Madison, WI 53705, USA

[f]University of Wisconsin Carbone Cancer Center, University of Wisconsin-Madison, Madison, WI 53705, USA

[g]Department of Surgery, School of Medicine and Public Health, University of Wisconsin-Madison, Madison, WI 53705, USA

Abstract

Mesenchymal stromal/stem cells (MSCs) are considered promising cellular therapeutics in the fields of tissue engineering and regenerative medicine. MSCs secrete high concentrations of immunomodulatory cytokines and growth factors, which exert paracrine effects on infiltrating immune and resident cells of the wound microenvironment that could favorably promote healing after acute injury. However, better spatial delivery and improved retention at the site of injury are two factors that could improve the clinical application of MSCs. In this study, we utilized thiol-ene Michael-type addition for rapid encapsulation of MSCs within a gelatin/poly(ethylene glycol) biomatrix; this biomatrix was also applied as a provisional dressing to full-thickness wounds in Sprague-Dawley rats. The three-way interaction of MSCs, gelatin/poly(ethylene glycol) biomatrices, and host immune cells and adjacent resident cells of the wound microenvironment favorably modulated wound progression and host response. In this model we observed attenuated immune cell infiltration, lack of foreign giant cell (FBGC) formation, accelerated wound closure

© 2013 Acta Materialia Inc. Published by Elsevier Ltd. All rights reserved.

*Corresponding author: W. John Kao, Ph.D., 777 Highland Avenue, 7123 Rennebohm Hall Madison, Wisconsin 53705, USA, WJKao@pharmacy.wisc.edu; Tel.: +1 608 263 2998; Fax: +1 608 262-5345, http://apps.pharmacy.wisc.edu/sopdir/PersonDetails.cfm?ID=36.
[1]Co-first author
Co-authors addresses: Kedi Xu and David A. Cantu, 777 Highland Avenue, 7232 Rennebohm Hall, University of Wisconsin-Madison, Madison, Wisconsin 53705, USA

Publisher's Disclaimer: This is a PDF file of an unedited manuscript that has been accepted for publication. As a service to our customers we are providing this early version of the manuscript. The manuscript will undergo copyediting, typesetting, and review of the resulting proof before it is published in its final citable form. Please note that during the production process errors may be discovered which could affect the content, and all legal disclaimers that apply to the journal pertain.

NIH-PA Author Manuscript
NIH-PA Author Manuscript
NIH-PA Author Manuscript

NIH-PA Author Manuscript

NIH-PA Author Manuscript

NIH-PA Author Manuscript

and re-epithelialization, as well as enhanced neovascularization and granulation tissue formation by 7 days. The MSC-entrapped gelatin/poly(ethylene glycol) biomatrix localized the presentation of MSCs adjacent to the wound microenvironment and thus, mediated early resolution of inflammatory events and facilitated proliferative phases in wound healing.

Keywords

cell encapsulation; foreign body response; mesenchymal stromal/stem cells; inflammation; monocyte/macrophages; wound healing

1 Introduction

Cell-based therapy is increasingly being used in clinical trials worldwide for treatment of acute tissue and organ injuries, degenerative diseases as well as congenital, metabolic, and immunological disorders [1], [2], and [3]. The development of clinical-grade cells (ie. highly processed biologicals) that meet FDA requirements of high purity, potency, safety, and efficacy for clinical applications is a challenging task [4]. Over the last decade, allogeneic mesenchymal stromal/stem cells (MSCs), have gained popularity using localized or systemic administration for treatment of various acute or chronic injuries and illnesses mainly due to their safe use as a third-party, off-the-shelf product [5]. Although previous studies have shown that MSCs migrate to inflamed tissue sites to promote healing, little is understood about the mechanism behind MSC homing and newer studies have shown limitations such as poor spatial delivery, short residence time (~24 hours), and low engraftment efficiency (<1%, after 7 days) [6] and [7]. The primary mechanism of MSC therapeutic action is also highly contested and includes transdifferentiation, direct differentiation, cell fusion, immune modulation, and secretion of potent trophic factors that enhance tissue repair [8], [9], and [10].

In the field of cutaneous wound repair, MSC carriers are increasingly being used to optimize cellular delivery adjacent to sites of injury and extend residence times to maximize MSC secretion of “pro-healing” molecules such as immumodulatory cytokines, pro-angiogenic and proliferative growth factors, and anti-fibrotic proteins [11]. Photo-polymerized semi-interpenetrating hydrogel networks composed of gelatin and poly(ethylene glycol) (PEG) diacrylate (PEGdA) were developed as provisional dressings that prevented infection, maintained wound hydration, and accelerated re-epithelialization [12], [13], and [14]. Subsequent formulations involved conjugation of L-cysteine to gelatin for thiol-ene polymerization to form interpenetrating networks that retained gelatin within crosslinked matrices [15]. Long-term incorporation of gelatin retained cell-adhesive sequences and collagenase- or matrix metalloproteinase (MMP)-sensitive sequences that facilitated focal adhesion formation and biomatrix remodeling respectively while extending the viability (28 days) of anchorage-dependent cells within three-dimensional hydrogels [16] and [17]. MSCs encapsulated in gelatin/poly(ethylene glycol) biomatrices also retained their multipotent (adipocyte, chondrocyte, and osteoblast differentiation) and immunomodulatory properties when cultured in the presence of biomatrix-adherent monocyte/macrophages [18]. In this study, a Michael-type addition reaction was utilized to enhance the applicability of this gelatin/poly(ethylene glycol) hydrogel platform, which does not require photoinitiator usage or external UV exposure [19].

Determining the biocompatibility of MSC-entrapped gelatin/poly(ethylene glycol) biomatrices must also be addressed to account for possible foreign body responses against the implanted biomaterial or adverse reactions to allogeneic MSCs. The variable concentration, composition, and conformation of adsorbed proteins on the biomaterial

NIH-PA Author Manuscript

NIH-PA Author Manuscript

NIH-PA Author Manuscript

implant could influence subsequent adhesion events of infiltrating immune cells and resident cells of the wound microenvironment. For example, excessive biomaterial surface activation can lead to a phenotypic switch in macrophages causing foreign body giant cell (FBGC) formation. FBGCs are multinucleated macrophages that damage implants by secreting acids, reactive oxygen species, and degradative enzymes. Likewise, cross-talk between biomaterial-adherent macrophages/FBGCs and fibroblasts or endothelial cells can also influence fibrous capsule formation or neovascularization respectively, which can impact the function of the MSC-entrapped biomatrix and the extent of wound resolution [20] and [21]. Allogeneic MSCs are generally considered to be non-immunogeneic due to the lack of expression of major histocompatibility complex (MHC) class II HLA-markers and co-stimulatory B7 molecules [22] and [23]. MSCs also secrete numerous immunomodulatory factors that inhibit T-, B-, and natural killer (NK)-cell proliferation and attenuate antigen-presenting cell activation [22] and [23]. Recent studies however have shown that interleukin-2-stimulated NK cells have a strong cytotoxic effect on allogeneic MSCs, while interferon-γ-activated MSCs can phagocytose large particles and act as antigen-presenting cells to CD4+ helper- and CD8+ cytotoxic-T cells [24]. We have previously demonstrated that encapsulated MSCs mediate the reprogramming of monocyte/macrophages to develop an anti-inflammatory phenotype favorable for wound healing [18] and [25]. Overall, MSC-entrapped biomatrices must promote wound resolution by enhancing neovascularization, re-epithelialization, and granulation tissue formation without inducing FBGC formation or causing excessive fibrosis.

2 Materials and Methods

2.1 Overview

Human MSCs used for *in vitro* three-dimensional culture studies were derived from de-identified donors as approved by the University of Wisconsin Hospital and Clinics Regulatory Committee (2011-345). Intramuscular injections, Sprague-Dawley rat bone marrow collection/culture, and cutaneous wound healing experiments were conducted in accordance to the guidelines set by and the Research Animal Resources Center (RARC) at the University of Wisconsin-Madison (M01829) and were in compliance with the NIH Guide for Care and Use of Laboratory Animals.

2.2 Synthesis and characterization of thiolated gelatin

Free thiols were conjugated to gelatin macromolecules (type B, bloom 225, Sigma-Aldrich, St. Louis, MO) by reacting gelatin lysyl residues, N-hydroxysuccinimide (NHS)-functionalized PEG (bis-NHS-PEG), and cysteamine to synthesize gelatin-PEG-thiol (gel-PEG-SH, Fig. 1A). All other chemicals were purchased from Sigma-Aldrich unless otherwise stated. Briefly, bis-NHS-PEG was synthesized via carbonate linkage between PEG-diol (2 kDa) and N, N′-disuccinimidyl carbonate (DSC, Acros Organics, Pittsburgh, PA) as previously reported [15]. Cysteamine was then reacted with N, N′-diisopropylethylamine (DIPEA) and 1 g of bis-NHS-PEG at a molar ratio of 1.2:1.2:1 respectively in dry dimethylformamide (DMF) under argon protection for 20 minutes at room temperature. A 1% gelatin/phosphate buffered saline solution (PBS, Invitrogen, Eugene, OR) (1:2 weight ratio of gelatin to bis-NHS-PEG) was added and stirred for 90 minutes with the pH adjusted to 8.0 by 1 N NaOH. Subsequently, 0.1 g of DL-Dithiothreitol (DTT) was added to the solution and stirred overnight to reduce disulfide bonds present in the synthesized gel-PEG-SH. The reaction mixture was then transferred to a Spectra/Por® Dialysis Membrane tube (12,000–14,000 Da molecular weight cutoff, Rancho Dominguez, CA) and dialyzed for 48 hours against pH 5.0 double-distilled water (ddH_2O)/HCl. The gel-PEG-SH solution was sterile filtered (0.22 μm), frozen (−80°C), and lyophilized. Gel-PEG-SH compound was characterized with a 400 MHz ^1H NMR spectrophotometer (Varian

NIH-PA Author Manuscript

NIH-PA Author Manuscript

NIH-PA Author Manuscript

Unity-Inova 400 MHz, Santa Clara, CA). The concentration of free thiol groups of gel-PEG-SH was determined by the Ellman's test using a 20% gel-PEG-SH/PBS (*w/w*) solution and absorbance was detected at 412 nm (spectrophotometer, Blk 800, Bio-Tek, Winooski, VT) and compared to an L-cysteine standard curve as previously described [15].

2. 3 Gelatin/poly(ethylene glycol) hydrogel preparation and characterization

Gelatin/poly(ethylene glycol) hydrogels were formed by a Michael-type thio-lene reaction between gel-PEG-SH and PEGdA. Various concentrations of gel-PEG-SH solutions (10%, 12.5%, and 15% *w/w*) were reacted with PEGdA solutions at different pH conditions (7.5, 8.5, or 9.5) with a thiol:acrylate molar ratio of 1:2 as optimized parameters for the reaction. The resultant pre-polymer solutions were thoroughly vortexed at room temperature and gelation was assessed by standard inversion with no flow observed within 30 seconds as the material selection criteria [26]. The rheological properties of the gelatin/poly(ethylene glycol) hydrogels (200 μL, pH 8.5 with 8%, 10%, 12% and 15% *w/w* gel-PEG-SH) were characterized by preparing the aforementioned solutions and transferring onto the rheometer plate (ARESLS2 2000ex, TA instruments, Schaumburg, IL). The precursor solution was kept on the plate for 30 min before the measuring gap size was adjusted to 1 mm. The storage modulus (G') and shear modulus (G'') were then recorded with the frequency-sweep mode of 0.1 Hz to 10 Hz and 2% strain at 25 °C as previously described [15]. For the swelling and degradation characterization, gelatin/poly(ethylene glycol) hydrogels (200 μL, pH 8.5, 10% gel-PEG-SH *w/w*) were similarly prepared in glass vials and allowed to gel at room temperature for an hour before immersing in 1 mL PBS. Samples were then incubated at 37°C and each hydrogel's weight was recorded at various time points after Kim Wipe surface drying. The swelling ratio was calculated as: (the weight of the swollen hydrogel/the initial weight of the hydrogel) × 100%. Degradation of the gelatin/poly(ethylene glycol) hydrogel was also assessed with similar preparation and pre-equilibration in PBS for 12 hours. Excess PBS was then carefully removed from the hydrogel using Kim Wipes and 1 mL of collagenase solution (0.1, 0.4, 1 mg/mL, 0.25–1.0 FALPA units/mg solid, type I-S from *Clostridium histolyticum*) was added to the hydrogel surface and incubated at 37°C. During hourly intervals, the weight of the remaining biomatrices (*Wt*) was recorded and fresh collagenase solutions were added until the hydrogel was completely degraded. The remaining weight fraction of the hydrogels for each time point was calculated as (*Wt/Wi*) × 100%, with *Wi* representing the hydrogel weight after the initial 12 hour PBS equilibration [27].

2.4 Three-dimensional in vitro human bone marrow-derived MSC encapsulation in gelatin/poly(ethylene glycol) biomatrix

Human bone marrow-derived mesenchymal stromal/stem cells (hBM-MSCs) were isolated from the bone marrow aspirate filters of de-identified healthy donors. Isolated hBM-MSC cells were cultured in standard MSC media consisting of Dulbecco's Modified Eagle Medium supplemented with non-essential amino acids (1X), 4 mM L-glutamine (Invitrogen, Eugene, OR), and 10% fetal bovine serum (FBS, Hyclone, Logan, UT). MSC identity was confirmed with MSC cell surface markers and lack of hematopoietic markers using CD29-PE, CD31-PE, CD34-FITC, CD44-PE, CD45-PE, CD54-PE, CD73-PE, CD90-APC (BD Biosciences, San Jose, CA), CD105-APC (eBiosciences, San Diego, CA, USA) monoclonal antibodies as previously described [18]. Only hBM-MSCs between passages 4–6 were used in the following *in vitro* study. Gel-PEG-SH was dissolved in PBS (12% w/w, 900 μL) with adjustment to pH 8.5 and lightly vortexed with a 50 μL cell suspension of 2×10^7 cells/mL of hBM-MSCs. The gel-PEG-SH/cell suspension was then mixed with 50 μL of a 30% (*w/w*) PEGdA solution and gently mixed by pipette with a final gel-PEG-SH concentration of 10% (*w/v*). The polymer/cell pre-cursor solution was then transferred into a 24-well cell culture plate (BD Biosciences) and was allowed to gel at room temperature for 30 minutes

NIH-PA Author Manuscript

NIH-PA Author Manuscript

NIH-PA Author Manuscript

before adding culture media. Similarly, cells were encapsulated in type I rat-tail collagen (4 mg/mL) after mixing with media, PBS (10x), and 1 N NaOH to form a neutralized solution or were entrapped within Matrigel® (2 mg/mL, BD Biosciences) following the manufacturer's instructions. The final concentration of cells for each hydrogel material was 1×10^6 cells/mL. Culture media was changed after 2 days and at 4 days, the gelatin/poly(ethylene glycol), type I collagen, and Matrigel® biomatrices were washed with PBS (2X) and incubated (37°C) with calcien-AM/ethidium homodimer (4μM/2μM, LIVE/DEAD®, Invitrogen, Grand Island, NY) for 30 minutes. The entrapped cells were subsequently imaged for viability using an epifluorescent microscope (Olympus TE300, Center Valley, PA) [15].

Retention of hBM-MSC differentiation capacity within three-dimensional gelatin/poly(ethylene glycol) biomatrices was assessed after culturing for 3 days in standard MSC culture media. Encapsulated MSCs were then released by digestion with collagenase (0.4 mg/mL), neutralized, rinsed with culture media, and pelleted after centrifugation (100xg, 5 minutes) for complete cell extraction from the supporting gelatin/poly(ethylene glycol) biomatrix. The hBM-MSCs were then re-plated on glass coverslips and cultured in 6-well tissue culture polystyrene plates (BD Biosciences) with standard MSC media until confluence (4–5 days) was attained. The culture media was then switched to Adipo NHdiff (16 days), Chondro NHdiff (16 days), or Osteo NHdiff medium® (14 days) (Miltenyi Biotec Inc., Auburn, CA) to induce MSC multidifferentiation into adipocytes, chondrocytes, and osteoblasts respectively. hBM-MSCs were detected for standard adipocyte, chondrocyte, osteoblast MSC differentiation via Oil red-O (lipid vacuoles), Safranin-O (glycosaminoglycans), and von Kossa (calcium deposits) staining respectively [18] and [28].

2.5 Intramuscular injection of gelatin/poly(ethylene glycol) hydrogels

Gelatin/poly(ethylene glycol) solution with the following parameters (200 μL, pH 8.5, gel-PEG-SH at 10% *w/w* and PEGdA at 1% *w/w*) was previously selected due to the mild reaction conditions and optimized polymerization time (~2 minutes), and was injected into the left thigh muscle of isoflurane anaesthetized (1.5% isoflurane, oxygen 1.5%) female Sprague-Dawley rats (250–300 g, 3 months old) using a 23-gauge needle. The rats also received a subcutaneous injection (1 mL) of meloxicam (1 mg/kg, St. Joseph, MO) analgesic. At 1, 4, and 7 days, the rats were euthanized with CO_2 asphyxiation and the whole muscle was isolated and fixed in 10% neutral buffered formalin for 48 hours, paraffin embedded, and stained in hematoxylin and eosin (H&E). Gross histological images were taken to assess the stability of the gelatin/poly(ethylene glycol) hydrogel and characterize foreign body response after injection.

2.6 Application of MSC-gelatin/poly(ethylene glycol) biomatrices in cutaneous wounds

Female Sprague-Dawley rats (250–300 g, 3 months old) were grouped into 3 different cohorts (n = 3 rats per treatment type for each time point) that were either left untreated as a sham control, treated with the gelatin/poly(ethylene glycol) hydrogel, or treated with the combined MSC-gelatin/poly(ethylene glycol) biomatrix. Sprague-Dawley rat MSCs (bone marrow-derived) were similarly isolated, cultured, and characterized as described for hBM-MSCs [29]. MSC passages (4–6) were used for this *in vivo* study. Full-thickness wounds were created on the dorsum of shaved and Betadine-prepped Sprague-Dawley rats using 8-mm biopsy punches (Miltex GmbH, York, PA) while under isoflurane anesthesia (1.5% isoflurane, oxygen 1.5%). Silicone rings (McMaster-Carr, Atlanta, GA) were glued down with Vetbond™ (3M, St. Paul, MN) by carefully placing the Vetbond™-coated silicone ring around the wound perimeter and firmly applying pressure for 2 minutes. The silicone rings were sutured (Nylon 4.0, Ethicon, Sun Prairie, WI) to inhibit healing by contraction, which is the accepted method for healing full-thickness wounds in rats [30] and [31]. Gelatin/

NIH-PA Author Manuscript

NIH-PA Author Manuscript

NIH-PA Author Manuscript

poly(ethylene glycol) hydrogels (400 μL) or MSC-gelatin/poly(ethylene glycol) biomatrices (400 μL, 1×10^6 Sprague-Dawley rat MSCs/mL) were similarly prepared as mentioned before and quickly applied to the full-thickness wounds. Rats also received a subcutaneous injection of meloxicam as previously described. After gelation (~1–2 minutes), all wounds were covered with Tegaderm™ film (3M) and then rats were wrapped with brown cling gauze followed by Vetrap™ (3M) tape. At 4 and 7 days, rats were euthanized with CO_2 asphyxiation, wounds were photographed, wound tissue was harvested (5×5 cm^2 area), fixed in 10% neutral buffered formalin for 48 hours, paraffin embedded, and H&E stained. Wound closure was assessed by measuring the wound sizes from digital photographs taken immediately after surgery and 4 or 7 days post-treatment and was calculated as the wound closure percentage [((area of original wound − area of healing wound)/area of original wound) × 100%] using Image J (NIH, USA) as previously described [32]. Photomicrographs were also taken of histological sections using a cross-section taken from the center of the wound area to assess epidermal maturity, neovascularization, and dermal remodeling of the rat skin wound tissue. Epidermal thickness of healing wound tissue with clearly demarcated epidermal and dermal tissue boundaries were measured by averaging five epithelialized keratinocyte widths from randomized locations including the central region of the wound and areas adjacent to the wound margin. The number of infiltrating keratinocytes, fibroblasts, mononuclear cells, and polymorphonuclear (PMN) leukocytes at the center of the wound and at the wound margin were differentiated morphologically, counted, and normalized to the observed wound areas for all treatment groups [12] and [13].

2.7 CD68 and CD163 immunochemistry (IHC) staining of macrophages within rat skin wound tissue

Paraffin-embedded rat skin wound tissue near the center of the wound was sectioned (5 μm) and incubated at 80°C for 20 minutes. Sections were deparraffinized in xylene (3 washes) and then hydrated though a graded ethanol series to deionized water. Antigen retrieval was performed in citrate buffer, pH 6.0 (10 mM citric acid, 0.05% tween 20) or Tris-Ethylenediaminetetraacetic acid (EDTA), pH 9.0 (10 mM tris base, 1 mM EDTA, 0.05% Tween 20) for 3 minutes in a Biocare decloaker (Biocare Medical, Concord, CA) and sections were allowed to cool for 30 minutes. After washing the sections with PBS, endogenous peroxidase activity was blocked with 3% hydrogen peroxide (H_2O_2) in PBS for 20 minutes. Sections were sequentially blocked with 10% goat serum (1 hour), 0.001% avidin (10 minutes), and 0.001% biotin (10 minutes) in PBS. Mouse anti-rat CD68 primary antibody (Serotec, Raleigh, NC) was diluted (1:800) in PBS containing 1% goat serum and 0.01% Triton X-100 and incubated overnight at 4°C. Mouse anti-rat CD163 primary antibody (Serotec) was similarly diluted (1:50) in PBS containing 1% goat serum and 0.01% Triton-X 100 overnight at 4°C. Afterwards, sections were washed with PBS (3 times) and reacted with SignalStain® Boost IHC Detection Reagent Horse Radish Peroxidase (HRP), Mouse (Cell Signaling Technologies, Danvers, MA) for polymer-based recognition of mouse IgG (primary antibody) for 30 minutes. Sections were rinsed again in PBS (3 times) and then reacted with a 3,3′-diaminobenzidine (DAB) solution (Vector Laboratories, Burlingame, CA) containing H_2O_2 to produce a dark brown reaction product for IHC detection of CD68 or CD163. Sections were rinsed with tap water and counterstained with Mayer's hematoxylin (1 minute). Afterwards the sections were rinsed in tap water and distilled water, dehydrated through a graded ethanol series to xylene, and coverslipped with permount (Fischer Scientific, Hampton, New Hampshire) for microscope visualization. Infiltrating macrophages that were $CD68^+$ (a pan macrophage marker) or $CD163^+$ (an anti-inflammatory (M2) macrophage marker) were counted and normalized to the observed wound areas for all treatment groups. The M2 percentage (indicating the percentage of anti-inflammatory macrophages) was calculated as [($CD163^+$ cells/$CD68^+$ cells) × 100%] as referenced [33].

NIH-PA Author Manuscript

NIH-PA Author Manuscript

NIH-PA Author Manuscript

2.8 Statistical Analysis

All values were expressed as the mean ± SD. Analysis of variance was used for multiple group comparison of samples between different cohorts (ie. sham wound, gelatin/poly(ethylene glycol) hydrogel, or MSC-gelatin/poly(ethylene glycol) biomatrix) for each time point (4 or 7 days). A student's t-test was also employed to assess the statistical significance between subjects of the same cohort for different time points (4 or 7 days). A probability value $p < 0.05$ was considered statistically significant.

3. Results

3.1 Gelatin/poly(ethylene glycol) hydrogel characterization

Thiolated gelatin molecules were prepared in a two step reaction (Fig. 1A) with synthesized bis-NHS-PEG compounds modified with cysteamine and conjugated to lysyl residues on the gelatin macromolecules. Cysteamine was utilized instead of L-cysteine due its higher solubility in dry DMF and greater Michael-type reaction efficiency needed for rapid gel formation. The development of disulfide bonds was minimized by reduction in excess amounts of DTT and the reaction mixture was dialyzed against pH 5.0 double-distilled deionized water to remove unwanted side products. Type B gelatin (bloom 225, 50,000–100,000 Da) was selected for the reaction to ensure that sufficient lysyl residues were present for conjugation and because the significant difference in molecular weight between gelatin and bis-NHS-PEG derivatives more easily facilitated purification of the final product (gel-PEG-SH) via dialysis. The structure of gel-PEG-SH was confirmed by ^{1}H NMR spectroscopy. The typical peaks of the gelatin molecule were observed (type B, bloom 225) with a broad peak at δ3.64 ppm due to the methylene protons present on the PEG constituent (position 1) while peaks at δ3.25 ppm (position 2) and δ2.59 ppm (position 3) were observed for the methylene protons present on the cysteamine moieties (Fig. 1B). The free thiol concentration for gel-PEG-SH was 227.0 ± 28.1 μmol/g (n = 5 different batches) as determined by the Ellman's test. Hydrogel gelation was optimized by testing three different polymer concentrations and pH levels with the molar ratio of gel-PEG-SH to PEGdA kept at 1.2 (Table 1).

After PBS immersion, the gelatin/poly(ethylene glycol) hydrogels rapidly swelled within 24 hours (an increase in the swelling ratio by 250%). The swelled hydrogels reached a plateau and remained relatively constant (250%–300%, 5 additional days). After 6 days, the hydrogels quickly lost bulk stability (as measured by a loss in weight) and were completely degraded after 9 days (Fig. 2A). Non-enzymatic degradation of the hydrogels was primarily due to the hydrolytic cleavage of the ester bonds between the gelatin backbone and thiol-ether groups present on the PEGdA component as previously described [34] and [35]. Gelatin/poly(ethylene glycol) hydrogels were also susceptible to enzymatic degradation after incubation with type I collagenase and varied in degradation time from 4 to 6 hours depending on the concentration utilized (0.1, 0.4, or 1 mg/mL type I collagenase, Fig. 2B). When comparing Michael-type to photopolymerized gelatin/poly(ethylene glycol) hydrogels previously developed in our laboratory, complete degradation was achieved with the Michael-type hydrogel (involving only thiol-acrylate crosslinking), whereas the photopolymerized hydrogel (involving both thiol-acrylate and acrylate-acrylate crosslinking) remained incompletely degraded for an extended time frame [16]. The mechanical properties of the gelatin/poly(ethylene glycol) hydrogels correlated with an increasing polymer weight/weight percentage. An increase in the gel-PEG-SH concentration resulted in a higher storage modulus of 845 ± 90 Pa (pH 8.5, 15% *w/w* gel-PEG-SH) as compared to 92 ± 67 Pa (pH 8.5, 8% w/w gel-PEG-SH). Two hydrogels with intermediate gel-PEG-SH concentrations demonstrated a similar storage modulus: 478 ± 56 Pa (pH 8.5, 10% *w/w* gel-PEG-SH) versus 581 ± 92 Pa (pH 8.5, 12% *w/w* gel-PEG-SH, Fig. 2C).

NIH-PA Author Manuscript

NIH-PA Author Manuscript

NIH-PA Author Manuscript

3.2 3-D in vitro human bone marrow-derived MSC encapsulation

Viability of hBM-MSCs (1×10^6 cells/mL) encapsulated within gelatin/poly(ethylene glycol) biomatrices (pH 8.5, 10% *w/w* gel-PEG-SH) was assessed after 4 days of culture by incubating the biomatrices with calcien-AM and ethidium homodimer. hBM-MSCs remained viable and distributed homogenously within the gelatin/poly(ethylene glycol) biomatrix and retained a rounded morphology similar to Matrigel® whereas hBM-MSCs encapsulated within collagen developed a more spindle-shaped morphology similar to fibroblasts (Fig. 3A). The gelatin/poly(ethylene glycol) biomatrices did not display obvious contraction during the first 5 days of culture; however, the bulk hydrogel structure only remained intact for 8 days due to both hydrolysis and enzymatic degradation. To evaluate the retention of MSC properties within the gelatin/poly(ethylene glycol) biomatrices, MSCs were assessed for their ability to differentiate into three common lineages (adipocyte, chondrocyte, and osteoblast MSC differentiation). hBM-MSCs released from the gelatin/poly(ethylene glycol) biomatrices (after 3 days of culture), and subcultured to confluence maintained MSC multi-differentiation capacity after switching to adipogeneic, chondrogenic, or osteogenic medias as detected with Oil Red-O, Safranin-O, or Von Kossa staining respectively (Fig. 3B).

3.3 Intramuscular injection of gelatin/poly(ethylene glycol) hydrogel

The biocompatibility and stability of the gelatin/poly(ethylene glycol) hydrogel was also assessed after intramuscular injection of the pre-cursor solution into the left thigh of Sprague-Dawley rats. The mixed gel-PEG-SH/PEGdA pre-polymer solution gelled *in situ* and could be observed after 1 day subsequent to injection. Acute inflammation occurred with significant recruitment of PMNs and monocyte/macrophages, which bordered the gelatin/poly(ethylene glycol) hydrogel 1 day after receiving the intramuscular injection (Fig. 4). By day 3, the gelatin/poly(ethylene glycol) hydrogel was surrounded by fibroblasts, lymphocytes, and macrophages without the presence of FBGCs. At 1 week post-injection, the bulk hydrogel structure was degraded and only small remnants could be observed amongst the surrounding muscle tissue. Infiltrating macrophages, migrating fibroblasts, and endothelial cells with new granulation tissue and neovascularization were observed. Cell necrosis or apparent tissue damage were not observed after intramuscular injection.

3.4 MSC-gelatin/poly(ethylene glycol) biomatrices for cutaneous wound repair

Sprague-Dawley rat MSCs (passage 4) were negative for the hematopoietic marker CD45 and positive for the MSC markers CD90 and CD73 (BD Biosciences) as observed by flow cytometry (data not shown). All animals were healthy and did not show signs of undue stress or infection. Exudation was observed at 4 days for the sham wound and gelatin/poly(ethylene glycol) hydrogel treatment groups and remained within the silicone ring possibly due the presence of occlusive dressings such as Tegaderm™ film, gauze, and Vetrap coverings. Remnants of the hydrogel structure remained at the tissue interface at both 4 and 7 days with significant PMN and monocyte/macrophage localization at the hydrogel interface however, FBGCs were not observed (Supplemental Fig. 1). Images taken of the three treatment groups demonstrated similar wound closures at 4 days (sham wound: 17 ± 9 %; gelatin/poly(ethylene glycol) hydrogel: 24 ± 20 %; MSC-gelatin/poly(ethylene glycol) biomatrix: 12 ± 12 %) with no statistically significant differences (Fig. 5A, Supplemental Fig. 4). By 7 days, the sham wound closure showed modest wound closure (25 ± 18 %) while the gelatin/poly(ethylene glycol) hydrogel treatment (54 ± 7 %) and MSC-gelatin/poly(ethylene glycol) biomatrix treatment (66 ± 5 %) were more greatly improved. The MSC-gelatin/poly(ethylene glycol) biomatrix treatment also demonstrated a statistically greater ($p = 0.019$) wound closure % than the sham control wound at 7 days. Accelerated re-epithelialization was statistically greater for the gelatin/poly(ethylene glycol) hydrogel (6.17 ± 2 mm, $p = 0.011$) and the MSC-gelatin/poly(ethylene glycol) biomatrix treatments (6.59 ±

NIH-PA Author Manuscript

NIH-PA Author Manuscript

NIH-PA Author Manuscript

2 mm, p = 0.0041) when compared to the sham wound, which did not form an immature epithelial layer by 7 days (Fig. 5B, Fig. 6). For skin wound tissue at the center of the wound, the density of PMNs per total observed wound area was elevated for both the sham control (95 ± 159 cells/total observed area) and the gelatin/poly(ethylene glycol) treatment groups (94 ± 94 cells/total observed area) at 4 days and remained elevated at 7 days for the sham control (120 ± 122 cells/total observed area, while very little PMN infiltration was observed for the MSC-gelatin/poly(ethylene glycol) biomatrix treatment at either 4 (19 ± 10 cells/total observed area) or 7 days (2 ± 4 cells/total observed area, Fig. 6, Fig. 7A). At 4 days, mononuclear cell infiltration was statistically greater for the gelatin/poly(ethylene glycol) hydrogel treatment (1718 ± 260 cells/total observed area) as compared to the sham wound (1087 ± 244 cells/total observed area, p = 0.037) and the MSC-gelatin/poly(ethylene glycol) biomatrix (615 ± 176 cells/total observed area, p = 0.0037). The gelatin/poly(ethylene glycol) hydrogel treatment at 4 days (1718 ± 260 cells/total observed area, p = 0.011) was statistically greater than at 7 days (586 ± 345 cells/total observed area, Fig. 6, Fig. 7B) for the same treatment cohort. At 4 days, fibroblast infiltration was attenuated (not statistically significant) more for the MSC-gelatin/poly(ethylene glycol) biomatrix treatment (3053 ± 702 cells/total observed area, Fig. 6, Fig. 7C) than the other treatment groups (sham control, gelatin/poly(ethylene glycol) hydrogel). The MSC-gelatin/poly(ethyleneglycol) biomatrix was statistically greater in fibroblast number per total observed wound area by 7 days (3053 ± 702 cells/total observed area, p = 0.038, Fig. 6, Fig. 7C) as compared to the fibroblast number at 4 days for the same treatment cohort. Keratinocytes could not be identified for any of the treatment groups in the center of the wound at 4 days; however, keratinocyte number per total observed area by 7 days for both the gelatin/poly(ethylene glycol) hydrogel (3829 ± 760 cells/total observed area, p = 0.00095) and the MSC-gelatin/poly(ethylene glycol) biomatrix (4687 ± 758 cells/total observed area, p = 0.00043) were statistically greater than the sham control (no keratinocytes observed, Fig. 6, Fig. 7D). Images were also taken at the wound margin (Supplemental Fig. 2) and cell counts were normalized to the total observed wound area for all treatments at 4 and 7 days (Supplemental Fig. 3).

3.5 CD68 and CD163 immunochemistry staining of macrophages within rat skin wound tissue results

Rat skin tissue sections were taken in areas adjacent to the center of the wound due to technical issues associated with the heating and antigen retrieval steps in the IHC protocol, which accounts for the discrepancy in tissue organization between the gross histological (H&E) images and the immunostained skin tissues. Macrophages that stained positive for CD163 (an anti-inflammatory (M2) macrophage marker) were elevated in the both the sham control (1214 ± 309 cells/total observed area, p = 0.0064) and the MSC-gelatin/poly(ethylene glycol) biomatrix treatments (1464 ± 644 cells/total observed area, p = 0.039) at 4 days and were statistically greater than the same treatment groups, which attenuated in $CD163^+$ macrophage infiltration by 7 days (Fig. 8, Fig. 10A). Macrophages that stained positive for CD68 (a pan-macrophage marker) per total observed wound area in the gelatin/poly(ethylene glycol) hydrogel (2195 ± 173 cells/total observed area, p = 0.0028) and MSC-gelatin/poly(ethylene glycol) biomatrix treatment groups (2440 ± 773 cells/total observed area, p = 0.037) were elevated at 4 days and statistically greater than the sham control (Fig. 9, Fig. 10B). The $CD68^+$ cells per total observed wound area began to attenuate for the gelatin/poly(ethylene glycol) hydrogel and MSC-gelatin/poly(ethylene glycol) treatments by 7 days whereas the sham control demonstrated greater $CD68^+$ cell density (1933 ± 1306 cells/total observed area) as compared to the same treatment group at 4 days. The M2 percentage [($CD163^+$ cells/$CD68^+$ cells) × 100%] for the sham wound was statistically greater (122 ± 23%, p = 0.014) than the gelatin/poly(ethylene glycol) hydrogel treatment at 4 days and was also greater than the sham control treatment at 7 days (8.79 ± 1%, p = 0.0011, Fig. 10C).

NIH-PA Author Manuscript

NIH-PA Author Manuscript

NIH-PA Author Manuscript

4. Discussion

4.1 Rationale for MSC encapsulation within gelatin/poly(ethylene glycol) biomatrices

Multicomponent hydrogels containing both synthetic polymers and natural extracellular matrix (ECM) proteins or ECM-derived peptides are increasingly being used in tissue engineering and regenerative medicine as an alternative to fibrin-, hyaluronic acid-, or collagen-only biomaterial strategies to minimize batch-to-batch variability and to provide customized mechanical properties [36] and [37]. Development of biomatrices that can effectively encapsulate therapeutically beneficial cells and enhance their presentation and function require carefully tailored mechanical, cell-adhesive, degradative, and transport properties of the material for the specific injury or disease model *in vivo* [38] and [39]. Purified gel-PEG-SH was developed as a starting product to facilitate rapid thiol-ene Michael-type hydrogel formation with PEGdA at mildly basic conditions for MSC encapsulation without UV or photoactivated polymerization as those modalities rely on the use of small molecule photoinitiators that generate cytotoxic free radicals [40] and [41]. Michael-type crosslinking of gel-PEG-SH derived from denatured bovine collagen (type B, bloom 225) with biologically inert PEGdA served the dual purpose of providing biochemical contact sites for anchorage-dependent MSCs while facilitating both passive dissolution and enzymatic degradation mechanisms that more closely mimicked cell-mediated ECM remodeling that occurs *in vivo* [42] and [43]. The high swelling ratio observed for the gelatin/poly(ethylene glycol) biomatrix was considered favorable for passive diffusion of MSC-secreted therapeutic proteins to adjacent wound tissue as previously described [44] and [45].

4.2 Retention of MSC properties in gelatin/poly(ethylene glycol) hydrogels and in vivo biocompatibility

MSCs encapsulated within the gelatin/poly(ethylene glycol) biomatrix showed high viability likely due to the mild gel polymerization conditions and the retention of the gelatin component facilitating adhesion for anchorage-dependent cells [15]. Entrapped MSCs displayed a more rounded morphology in the gelatin/poly(ethylene glycol) biomatrix compared with a more spread out spindle-shape in the type I collagen hydrogel. Such observations were most likely due to differences in the stiffness, distribution and conformation of specific cell-adhesive ligands, and the ability of the MSCs to apply mechanical forces to the surrounding matrix [46]. Cell shape is also an important regulator of cell behavior with biomatrices that could serve as a niche causing MSCs to develop a spherical morphology, switch MSCs into a quiescent state, and preserve their multilineage potential while MSCs encapsulated within collagen developed fusiform morphologies and demonstrated greater cell-mediated contraction of the biomatrix as observed *in vitro* [47]. The gelatin/poly(ethylene glycol) hydrogel induced an acute inflammatory response characterized by significant PMN and monocyte/macrophage infiltration that attenuated with time after intramuscular injection or hydrogel application to full-thickness wounds. The relatively short time frame that the gelatin/poly(ethylene glycol) hydrogel remained intact after intramuscular injection may have also contributed to a lack of FBGC localization or fibrous encapsulation at tissue-material interface [20]. The material properties of the gelatin/poly(ethylene glycol) hydrogel may have resisted FBGC formation as gelatin is a denatured natural ECM component that is amenable to proteolytic remodeling and rarely induces chronic inflammation and poly(ethylene glycol) tends to resist non-specific protein adsorption that could otherwise promote biomaterial-mediated phenotypic switching in infiltrating monocyte/macrophages to favor FBGC formation and fibrous encapsulation [48]. The continued presence of PMNs at 7 days (Supplemental Fig. 1) at the hydrogel interface has also been linked with a lack of FBGC formation as demonstrated *in vitro* for direct contact biomaterial-PMN-monocyte/macrophage co-culture studies [49]. Although

NIH-PA Author Manuscript

NIH-PA Author Manuscript

NIH-PA Author Manuscript

monocyte/macrophages initially adhere to several types of materials, they often detach at later time points and undergo anoikis (adhesion-dependent cell death), a process that has been inversely correlated to FBGC formation. The lack of necrosis, FBGC formation, and fibrous encapsulation is indicative of the overall biocompatibility of the gelatin/poly(ethylene glycol) hydrogel [20].

4.3 Enhanced wound healing after treatment with the gelatin/poly(ethylene glycol) hydrogel or the MSC-gelatin/poly(ethylene glycol) biomatrix

Favorable re-epithelialization and wound closure at 7 days that were similarly observed for the gelatin/poly(ethylene glycol) hydrogel treatment and the MSC-gelatin/poly(ethylene glycol) biomatrix could be due to the material characteristics of the occlusive dressing for full thickness wounds which include: conformation to complex wound geometries, barrier function to provide mechanical protection and prevent bacterial infection, minimized fluid or heat loss, exudate absorbance, compression application to limit edema and dead wound space, non-adherence to wound tissues to reduce skin disruption after hydrogel removal, and a moist environment that enhances re-epithelialization as previously investigated [12], [13], and [14]. Topographical cues and MMP-susceptible moieties provided by the porous network of the three-dimensional gelatin/poly(ethylene glycol) hydrogel may have also facilitated a contact guidance effect that accelerated fibroblast infiltration into the wound defect from adjacent dermal tissues [50] and [51]. Elevated infiltration of PMNs and mononuclear cells at 4 days observed for the gelatin/poly(ethylene glycol) hydrogels without MSCs could be attributed to early surface-adherent immune cell activation that attenuated by 7 days; however, such localization did not appear to adversely influence downstream wound healing events as indicated by accelerated wound closure and re-epithelialization. The presence of gelatin within the gelatin/poly(ethylene glycol) network, which contains cell-adhesive moieties such as RGD, may have elicited less inflammation and a more modest host response as suggested by investigators involved in a subcutaneous implant study comparing PEG-only hydrogels and PEG-RGD modified hydrogels [52]. Topical application and the non-adhesiveness of the gelatin/poly(ethylene glycol) hydrogel may have also minimized an adverse foreign body response (characterized by FGBC formation and fibrous encapsulation) despite immune cell localization to hydrogel interface because the biomaterial did not remain permanently incorporated into the wound tissue and was displaced by infiltrating keratinocytes or fibroblasts by 7 days [48]. Inclusion of MSCs in the gelatin/poly(ethylene glycol) biomatrix appeared to have only a modest influence on the enhancement of final re-epithelialization and wound progression as compared to the gelatin/poly(ethylene glycol) hydrogel treatment group. As the encapsulating gelatin/poly(ethylene glycol) biomatrix remained intact during this study, possible engraftment and differentiation of MSCs into resident skin cell types did not likely represent a dominant mechanism by which MSCs promoted healing [53]. When in contact with the rat wound exudate, the swelling, dissolution, and biodegradation properties of the gelatin/poly(ethylene glycol) biomatrix may have also hindered effective diffusion of therapeutic MSC molecules and crucial juxtacrine interactions between MSCs and infiltrating phagocytes or resident cells of the wound microenvironment that have previously been shown to promote cutaneous tissue regeneration [11] and [54].

4.4 Differential macrophage phenotypic polarization amongst the different treatment groups

The $CD68^+$ (a pan macrophage marker) macrophage infiltration per observed wound area was elevated at 4 days for both the gelatin/poly(ethylene glycol) hydrogel and the MSC-gelatin/poly(ethylene glycol) biomatrix treatments as compared to the sham control, suggesting that the material and the encapsulated cells enhanced early macrophage recruitment to the material interface. Previous investigations that utilized TNF-α or hypoxia-

NIH-PA Author Manuscript

NIH-PA Author Manuscript

NIH-PA Author Manuscript

conditioned MSCs, which may potentially mimic conditions presented to encapsulated MSCs applied to full-thickness wounds, produced a plethora of chemoattractant molecules such as IL-6 and IL-8, macrophage inflammatory proteins (MIP-1, MIP-2), and monocyte chemotactic protein-1 (MCP-1). When concentrated MSC conditioned media was applied topically to cutaneous wounds, robust infiltration of the $CD68^+$ macrophages was similarly observed that was positively correlated to accelerated wound closure and re-epithelialization [55] and [56]. A prior *in vitro* investigation showed that monocyte/macrophages adherent to gelatin/poly(ethylene glycol) hydrogels induced elevated expression of TNF-α and IL-6 by 24 hours, which may contribute to greater $CD68^+$ macrophage recruitment to the wound bed [18]. The gelatin/poly(ethylene glycol) hydrogel system has also been shown to enhance IL-8 expression in a swine partial-thickness wound model, which could similarly attract $CD68^+$ macrophages but can also stimulate keratinocyte migration and proliferation leading to enhanced re-epithelialization at the wound bed [13] and [56]. The lower $CD68^+$ infiltration observed at 4 days for the sham control demonstrates a delay in macrophage recruitment possibly due to a lack of chemotactic signals either being released from the encapsulated MSCs or by the absence of a gelatin/poly(ethylene glycol) hydrogel to induce a mild foreign body response that stimulates macrophage chemotaxis to the hydrogel interface. Greater $CD163^+$ cell (an M2 macrophage marker) infiltration was elevated for both the sham control and the MSC-gelatin/poly(ethylene glycol) at 4 days as compared to 7 days. The M2% ($CD163^+$ cells/$CD68^+$ cells) was also most elevated for the sham control at 4 days. Although greater $CD163^+$ expression in infiltrating macrophage had previously been correlated to a more favorable healing outcome, this trend was not consistent in this investigation as the sham control demonstrated attenuated wound closure and incomplete re-epithelialization by 7 days [33] and [57]. Likewise, interpretation of the M2% ($CD163^+$ cells/$CD68^+$ cells) is complicated by the fact that the sham control exceeded 100% at 4 days. This discrepancy may be due to variable primary antibody affinity specific for CD163 and CD68 and inherent variability in macrophage infiltration between animal subject wound tissue for the different treatment cohorts. Specific tissue sections could also vary in the number of $CD163^+$ or $CD68^+$ cells depending on the location of the cross-section within the tissue (center of the wound versus adjacent to the wound perimeter). Overall, the number of $CD68^+$ macrophages present within the tissue rather than the number of $CD163^+$ macrophages appeared to more closely correlate with accelerated wound closure and re-epithelialization as observed for the gelatin/poly(ethylene glycol) and MSC-gelatin/poly(ethylene glycol) treatment groups.

Conclusion

We demonstrated that the application of gelatin/poly(ethylene glycol) hydrogels containing entrapped MSCs to injured skin accelerated wound closure and re-epithelialization and enhanced epidermal maturity, neovascularization, and granulation tissue formation. The interaction of encapsulated MSCs, gelatin/poly(ethylene glycol) hydrogels, infiltrating immune cells, and adjacent resident cells of the wound microenvironment impacted the course of wound progression and the overall host response in favor of cutaneous tissue regeneration.

Supplementary Material

Refer to Web version on PubMed Central for supplementary material.

NIH-PA Author Manuscript

NIH-PA Author Manuscript

NIH-PA Author Manuscript

Acknowledgments

We generously thank Beth Gray and Joe Hardin for their technical assistance in H&E histological processing and IHC characterization respectively. Research was supported in part by the University of Wisconsin-Madison School of Pharmacy.

References

1. Grim SA, Clark NM. Management of Infectious Complications in Solid-Organ Transplant Recipients. Nature. 2011; 90:333–342.
2. Daley GQ, Scadden DT. Prospects for Cell-Based Therapy. Cell. 2008; 132:544–548. [PubMed: 18295571]
3. Lechler RI, Sykes M, Thomson AW, Turka LA. Organ transplantation – how much of the promise has been realized? Nature. 2005; 11:605–613.
4. Halme DG, Kessler DA. FDA Regulation of Stem-Cell Based Therapies. New Eng J Med. 2006; 355:1730–1735. [PubMed: 17050899]
5. Parekkadan B, Milwid JM. Mesenchymal Stem Cells as Therapeutics. Annu Rev Biomed Eng. 2010; 12:87–117. [PubMed: 20415588]
6. Karp JM, Teo GSL. Mesenchymal Stem Cell homing: The Devil Is in the Details. Cell Stem Cell. 2009; 4:206–216. [PubMed: 19265660]
7. Hanson SE, Kleinbeck KR, Cantu D, Kim J, Bentz ML, Faucher LD, Kao WJ, Hematti P. Local delivery of allogeneic bone marrow and adipose tissue-derived mesenchymal stromal cells for cutaneous wound healing in a porcine model. J Tissue Eng Regen Med. 2013 [Epub ahead of print]. 10.1002/term.1700
8. Phinney DG, Prockop DJ. Concise Review: Mesenchymal Stem/Multipotent Stromal Cells: The State of Transdifferentiation and Modes of Tissue Repair – Current Views. Stem Cells. 2007; 25:2896–2902. [PubMed: 17901396]
9. Meirelles LDS, Fontes AM, Covas DT, Caplan AI. Mechanisms involved in the therapeutic properties of mesenchymal stem cells. Cyt Grow Fact Rev. 2009; 20:419–427.
10. Psaltis PJ, Zannettino ACW, Worthley SG, Gronthos S. Concise Review: Mesenchymal Stromal Cells: Potential for Cardiovascular Repair. Stem Cells. 2008; 26:2201–2210. [PubMed: 18599808]
11. Jackson WM, Nesti LJ, Tuan RS. Concise Review: Clinical Translation of Wound Healing Therapies Based on Mesenchymal Stem Cells. Stem Cells Trans Med. 2012; 1:44–50.
12. Kleinbeck KR, Faucher L, Kao WJ. Multifunctional In Situ Photopolymerized Semi-Interpenetrating Network System is an Effective Donor Site Dressing: A Cross Comparison Study in a Swine Model. J Burn Care Res. 2009; 30:37–45. [PubMed: 19131760]
13. Kleinbeck KR, Faucher LD, Kao WJ. Biomaterials modulated interleukin-8 and other inflammatory proteins during reepithelialization in cutaneous partial-thickness wounds in pigs. Wound Rep Reg. 2010; 18:486–498.
14. Xu K, Kleinbeck KR, Kao WJ. Multifunctional Biomaterial Matrix for Advanced Wound Healing. Adv Wound Care. 2012; 1:75–80.
15. Fu Y, Xu K, Zheng X, Giacomin AJ, Mix AW, Kao WJ. 3D cell entrapment in crosslinked thiolated gelatin-poly(ethylene glycol) diacrylate hydrogels. Biomaterials. 2012; 33:48–58. [PubMed: 21955690]
16. Xu K, Fu Y, Chung W, Zheng X, Cui U, Hsu IC, et al. Thiol-ene-based biological/synthetic hybrid biomatrix for 3-D living cell culture. Acta Biomaterialia. 2012; 8:2504–2516. [PubMed: 22484717]
17. Fu Y, Kao WJ. In situ forming poly(ethylene glycol)-based hydrogels via thiol-maleimide Michael-type addition. J Biomed Mater Res Part A. 2011; 98A:201–211.
18. Cantu DA, Hematti P, Kao WJ. Cell encapsulating biomaterial regulates MSC differentiation and macrophage immunophenotype. Stem Cell Trans Med. 2012; 1:740–749.
19. Patterson J, Martino MM, Hubbell JA. Biomimetic materials in tissue engineering. Mater Today. 2010; 13:14–22.

NIH-PA Author Manuscript

NIH-PA Author Manuscript

NIH-PA Author Manuscript

20. Anderson JM, Rodriguez, Chang DT. Foreign Body Reaction to Biomaterials. Semin Immunol. 2008; 20:86–100. [PubMed: 18162407]
21. Badylak SF, Gilbert TW. Immune Response to Biologic Scaffold Materials. Semin Immunol. 2008; 20:109–116. [PubMed: 18083531]
22. Tolar J, Le Blanc K, Keating A, Blazar BR. Concise review: hitting the right spot with mesenchymal stromal cells. Stem Cells. 2010; 28:1446–1455. [PubMed: 20597105]
23. Battiwalla M, Hematti P. Mesenchymal stem cells in hematopoietic stem cell transplantation. Cytotherapy. 2009; 11:503–15. [PubMed: 19728189]
24. Stagg J. Immune regulation by mesenchymal stem cells: two sides to the coin. Tissue Antig. 2007; 69:1–9.
25. Kim J, Hematti P. Mesenchymal stem cells-educated macrophages: A novel type of alternatively activated macrophages. Exp Hematol. 2009; 37:1445–1453. [PubMed: 19772890]
26. Kuo CK, Ma PX. Ionically crosslinked alginate hydrogels as scaffolds for tissue engineering: Part 1. Structure gelation rate and mechanical properties. Biomaterials. 2001; 22:511–521. [PubMed: 11219714]
27. Benton JA, Deforest CA, Vivekanandan V, Anseth KS. Photocrosslinking of Gelatin Macromers to Synthesize Porous Hydrogels That Promote Valvular Interstitial Cell Function. Tissue Eng Part A. 2009; 15:3221–3230. [PubMed: 19374488]
28. Chan BP, Hui TY, Yeung CW, Li J, Mo I, Chan GCF. Self-assembled collagen-human mesenchymal stem cell microspheres for regenerative medicine. Biomaterials. 2007; 28:4652–4666. [PubMed: 17681374]
29. Trivedi P, Hematti P. Derivation and immunological characterization of mesenchymal stromal cells from human embryonic stem cells. Exp Hematol. 2008; 36:350–359. [PubMed: 18179856]
30. Lindblad WJ. Considerations for selecting the correct animal model for dermal wound healing studies. J Biomater Sci Poly Ed. 2008; 19(8):1087–1096.
31. Dorsett-Martin WA. Rat models of skin wound healing: A review. Wound Rep Reg. 2004; 12(6): 591–599.
32. Wu Y, Chen L, Scott PG, Tredget EE. Mesenchymal Stem Cells Enhance Wound Healing Through Differentiation and Angiogenesis. Stem Cells. 2007; 25:2648–2659. [PubMed: 17615264]
33. Brown BN, Valentin JE, Stewart-Akers AM, McCabe GP. Macrophage phenotype and remodeling outcomes in response to biologic scaffolds with and without a cellular component. Biomaterials. 2009; 30:1482–1491. [PubMed: 19121538]
34. Jin R, Teixeira LSM, Krouwels A, Dijkstra PJ, Blitterswijk CAV, Kaperien M, et al. Synthesis and characterization of hyaluronic acid-poly(ethylene glycol) hydrogels via Michael addition: An injectable biomaterial for cartilage repair. Acta Biomaterialia. 2010; 6:1968–1977. [PubMed: 20025999]
35. Shu XZ, Ahmad S, Liu Y, Prestwich GD. Synthesis and evaluation of injectable, in situ crosslinkable synthetic extracellular matrices for tissue engineering. J Biomed Mater Res Part A. 2006; 79:902–912.
36. Parenteau-Bariel R, Gauvin R, Berthod F. Collagen-Based Biomaterials for Tissue Engineering Applications. Mater. 2010; 3:1863–1887.
37. Discher DE, Mooney DJ, Zandstra PW. Growth factors, Matrices, and Forces Combine and Control Stem Cells. Science. 2009; 324:1673–1677. [PubMed: 19556500]
38. Seliktar D. Designing Cell-Compatible hydrogels for Biomedical Applications. Science. 2012; 336:1124–1128. [PubMed: 22654050]
39. Lutolf MP, Hubbell JA. Synthetic biomaterials as instructive extracellular microenvironments for morphogenesis in tissue engineering. Nature Biotech. 2005; 23(1):47–55.
40. Fedorovich NE, Oudshoorn MH, Geemen DV, Hennink WE, Alblas J, Dhert WJA. The effect of photopolymerization on stem cells embedded in hydrogels. Biomaterials. 2009; 30:344–353. [PubMed: 18930540]
41. Nicodemus GD, Bryant SJ. Cell encapsulation in Biodegradable Hydrogels for Tissue Engineering Applications. Tissue Eng: Part B. 2008; 14:149–165.

NIH-PA Author Manuscript

NIH-PA Author Manuscript

NIH-PA Author Manuscript

42. Heino J, Huhtala M, Käpyla J, Johnson MS. Evolution of collagen-based adhesion systems. Int J Biochem Cell Bio. 2009; 41:341–348. [PubMed: 18790075]
43. Waldeck H, Kao WJ. Effect of the Addition of a Labile Gelatin Component on the Degradation and Solute Release Kinetics of a Stable PEG hydrogel. J Biomat Sci. 2012; 23:1595–1611.
44. Fu Y, Kao WJ. Drug Release Kinetics and Transport Mechanisms from Semi-interpenetrating Networks of Gelatin and Poly(ethylene glycol) diacrylate. Pharm Res. 2009; 26:2115–2124. [PubMed: 19554430]
45. Kleinbeck KR, Bader RA, Kao WJ. Concurrent In Vitro Release of Silver Sulfadiazine Bupivacaine From Semi-interpenetrating Network for Wound Management. J Burn Care Res. 2009; 30:98–104. [PubMed: 19060724]
46. Geiger B, Spatz JP, Bershadsky AD. Environmental sensing through focal adhesions. Nat Rev. 2009; 10:21–33.
47. Guilak F, Cohen DM, Estes BT, Gimble JM, Liedtke W, Chen CS. Control of Stem Cell Fate by Physical Interactions with the Extracellular Matrix. Cell Stem Cell. 2009; 5:17–26. [PubMed: 19570510]
48. Franz S, Rammelt S, Scharnweber D, Simon JC. Immune response to implants – A review of the implications for the design of immunomodulatory biomaterials. Biomaterials. 2011; 32:6692–6709. [PubMed: 21715002]
49. Kirk JT, McNally AK, Anderson JM. Polymorphonuclear Leukocyte Inhibition of Monocytes/Macrophages in the Foreign Body Reaction. J Biomed Mater Res Part A. 2010; 94:683–687.
50. Kim HN, Hong Y, Kim MS, Kim SM, Suh K-Y. Effect of orientation and density of nanotopography in dermal wound healing. Biomaterials. 2012; 33:8782–8792. [PubMed: 22959181]
51. Raeber GP, Lutolf MP, Hubbell JA. Molecularly Engineered PEG Hydrogels: A Novel System for Proteolytically Mediated Cell Migration. Biophys J. 2005; 89:1374–1388. [PubMed: 15923238]
52. Lynn AD, Kyriakides TR, Bryant SJ. Characterization of the in vitro macrophage response and in vivo host response to poly(ethylene glycol)-based hydrogels. J Biomed Mater Res Part A. 2010; 93A:941–953.
53. Sasaki M, Abe R, Fujita Y, Ando S, Inokuma D, Shimizu H. Mesenchymal stem cells are recruited into wounded skin and contribute to wound repair by transdifferentiation into multiple skin cell types. J Immunol. 2008; 180:2581–2587. [PubMed: 18250469]
54. Boateng JS, Matthews KH, Stevens HNE, Eccleston GM. Wound Healing Dressings and Drug Delivery Systems: A Review. J Pharm Sci. 2008; 97:2892–2923. [PubMed: 17963217]
55. Chen L, Tredget EE, Wu PYG, Wu Y. Paracrine Factors of Mesenchymal Stem Cells Recruit Macrophages and Endothelial Lineage Cells and Enhance Wound Healing. PloS ONE. 2008; 3:e1886. [PubMed: 18382669]
56. Heo SC, Jeon ES, Lee IH, Kim HS, Kim MB, Kim JH. Tumor Necrosis Factor-α-Activated Human Adipose Tissue-Derived Mesenchymal Stem Cells Accelerate Cutaneous Wound Healing through Paracrine Mechanisms. J Inv Derm. 2011; 131:1559–1567.
57. Badylak SF, Valentin JE, Ravindra AK, McCabe GP, Stewart-Aker AM. Macrophage Phenotype as a Determinant of Biologic Scaffold Remodeling. Tissue Eng: Part A. 2008; 14:1835–1842. [PubMed: 18950271]

NIH-PA Author Manuscript

NIH-PA Author Manuscript

NIH-PA Author Manuscript

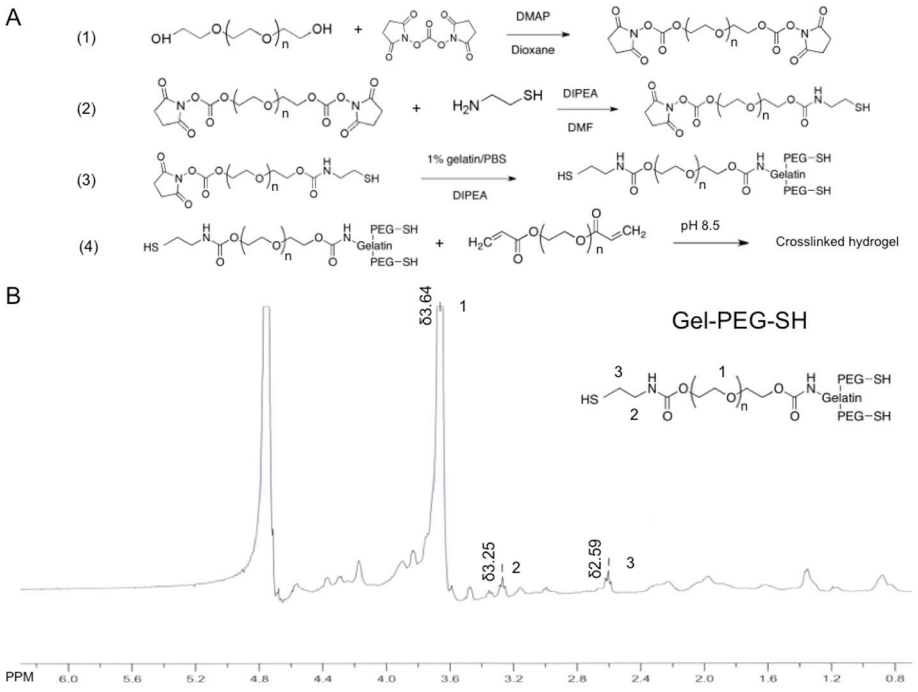

Figure 1.

Synthesis and characterization of thiolated gelatin.

A: Synthesis procedure of thiolated gelatin macromolecule with a two-step reaction between lysyl residue of gelatin, cysteamine and PEG-bis-NHS linker. (1) Synthesis of PEG-bis-NHS via a carbonate linker. (2) Synthesis of thiol modified PEG (NHS-PEG-SH). (3) Synthesis of thiol modified gelatin (type B gelatin, bloom 225) (gel-PEG-SH). (4) Crosslinking of thiol modified gelatin (gel-PEG-SH) with PEGda via Michael-type addition.

B: ^{1}H NMR of the thiolated gelatin (type B, bloom 225, Gel-PEG-SH).

NIH-PA Author Manuscript

NIH-PA Author Manuscript

NIH-PA Author Manuscript

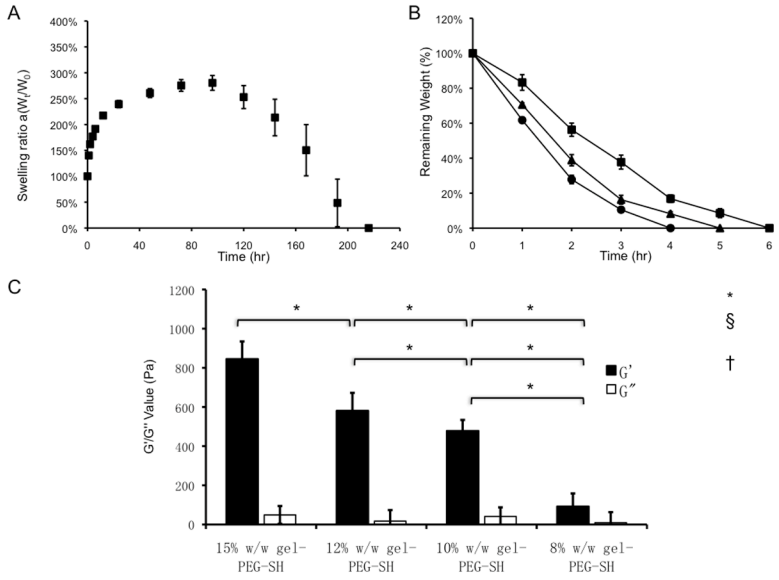

Figure 2.

Gelatin/poly(ethylene glycol) hydrogel bulk characterization.

A: Swelling characterization of 10% gelatin/poly(ethylene glycol) biomatrices (n = 3) immersed in PBS at 37°C.

B: Enzymatic degradation of 10% gelatin/poly(ethylene glycol) biomatrices (n = 3) by type I collagenase (collagenase concentrations: ▪: 0.1mg/mL, ▲: 0.4 mg/mL, ●: 1 mg/mL).

C: Rheological characterization of gelatin/poly(ethylene glycol) hydrogels with various polymer concentrations (G′ ■ storage modulus and G″ □ shear modulus at pH 8.5, 15%w/w gel-PEG-SH; at pH 8.5, 12% w/w gel-PEG-SH; at pH 8.5, 10% w/w gel-PEG-SH; at pH 8.5, 8% w/w gel-PEG-SH.) G′ ■ at pH 8.5, 15% w/w gel-PEG-SH was statistically greater than all other gel-PEG-SH concentrations); G′ ■ at pH 8.5, 12% w/w gel-PEG-SH was statistically greater than 10% w/w gel-PEG-SH and 8% w/w gel-PEG-SH; G′ ■ at pH 8.5, 10% w/w gel-PEG-SH was statistically greater than 8% w/w gel-PEG-SH. G″ was not statistically significant amongst different polymer concentrations. *p <0.001.

NIH-PA Author Manuscript

NIH-PA Author Manuscript

NIH-PA Author Manuscript

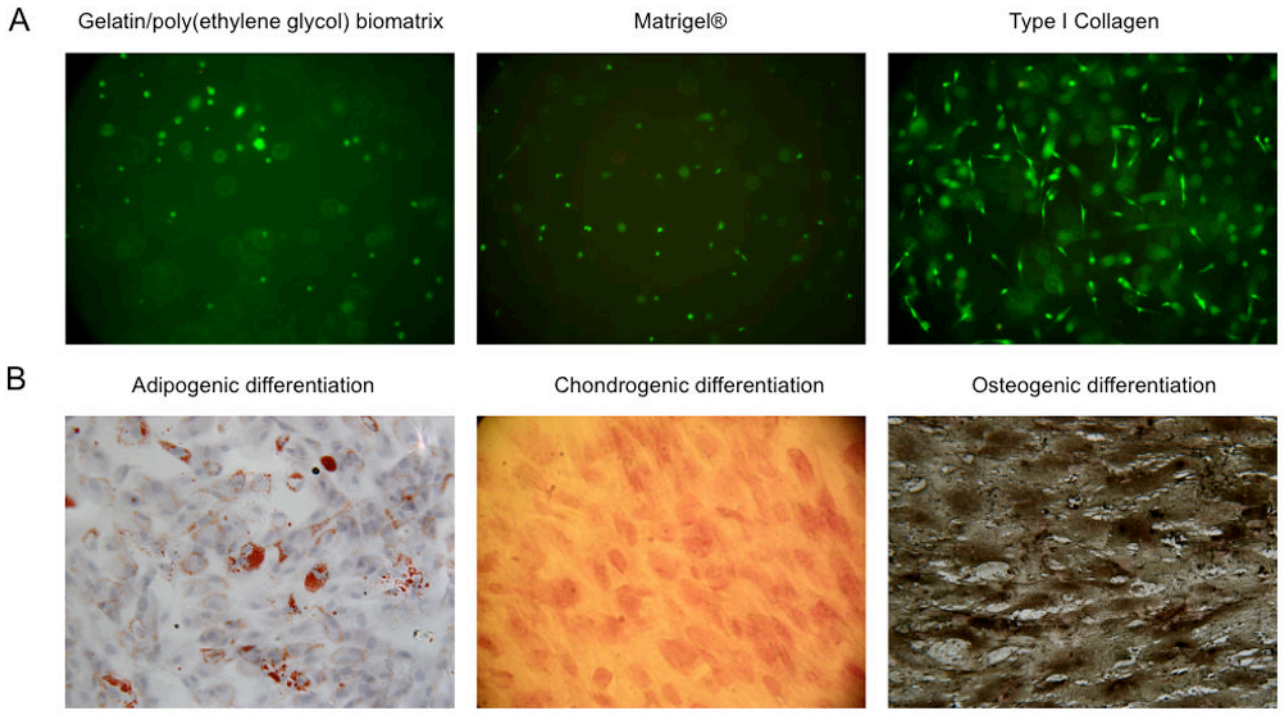

Figure 3.

3D cell encapsulation viability evaluation and the retention of hBM-MSC differentiation capability.

A: LIVE/DEAD® staining of hBM-MSCs encapsulation within a gelatin/poly(ethylene glycol) biomatrix, Matrigel®, or type I collagen for 4 days (20x magnification).

B: hBM-MSC were encapsulated in gelatin/poly(ethylene glycol) biomatrices for 3 days and released by collagenase digestion. After re-plating and growing to confluency, hBM-MSC were switched to separate differentiation medias and were subsequently tested for adipocyte-, chondrocyte-, osteoblast-lineage differentiation after 16 days (left), 16 days (middle), 14 days (right) respectively (20x magnification). Oil red O–staining shows lipid droplets (left: red color), Safranin-O staining shows cartilage-specific glycosaminoglycans (middle: reddish-pink ECM), von Kossa staining shows deposits of calcium crystals (right: black dots).

NIH-PA Author Manuscript

NIH-PA Author Manuscript

NIH-PA Author Manuscript

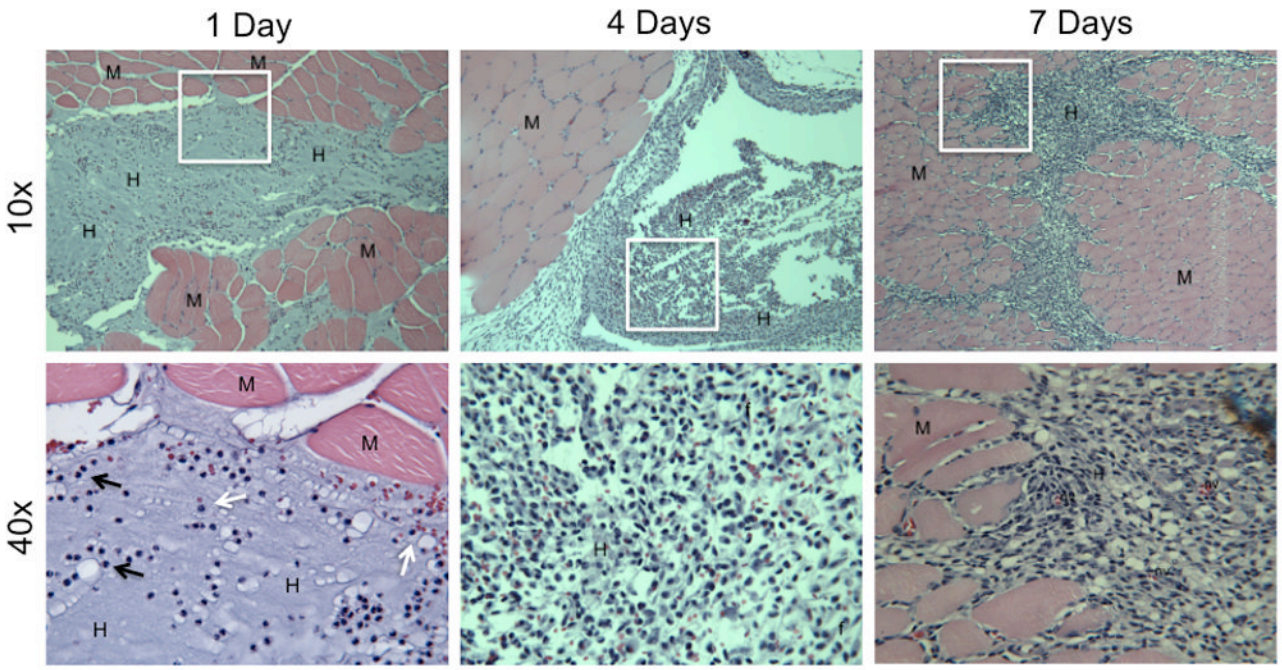

Figure 4.

Representative histological sections of intramuscular injections with gelatin/poly(ethylene glycol) hydrogels for 1, 4, and 7 days (both 10x and 40x magnification). M = muscle; H = remnants of the gelatin/poly(ethylene glycol) hydrogel; F = fibroblast; NV = neovascularization; black arrows = PMNs; white arrows = monocyte/macrophages.

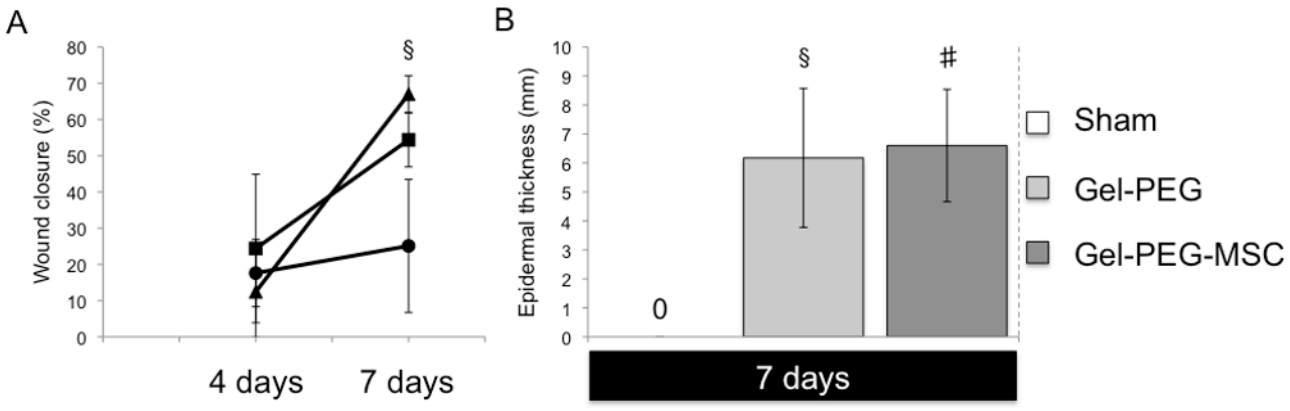

Figure 5.

Wound closure and extent of re-epithelialization

A: The wound closure (%) means ± SD (N = 3) observed for three different treatment groups (sham wound ●, gelatin/poly(ethylene glycol) hydrogel ■, and MSC-gelatin/poly(ethylene glycol) biomatrix ▲) after 4 or 7 days post-surgery. Wound closure (%) was calculated as: [(original wound area - wound area post-surgery)/original wound area] x100%. A probability $p < 0.05$ was considered statistically significant using student's t-test. The MSC-gelatin/poly(ethylene glycol) biomatrix treatment demonstrated greater wound closure than the sham control (§$p = 0.019$) at 7 days.

B: 7 day full-thickness wounds for sham = sham control (no observed re-epithelialization), Gel-PEG = gelatin/poly(ethylene glycol) hydrogel, Gel-PEG-MSC = MSC-gelatin/poly(ethylene glycol) biomatrix. A total of 5 widths were taken at random locations within the wound and averaged, the means ± SD were taken into account amongst the groups (n = 3). Both the gelatin/poly(ethylene glycol) hydrogel (§$p = 0.011$) and the MSC-gelatin/poly(ethylene glycol) biomatrix (#$p = 0.0041$) demonstrated statistically greater epidermal thickness than the sham control at 7 days.

NIH-PA Author Manuscript
NIH-PA Author Manuscript
NIH-PA Author Manuscript

NIH-PA Author Manuscript
NIH-PA Author Manuscript
NIH-PA Author Manuscript

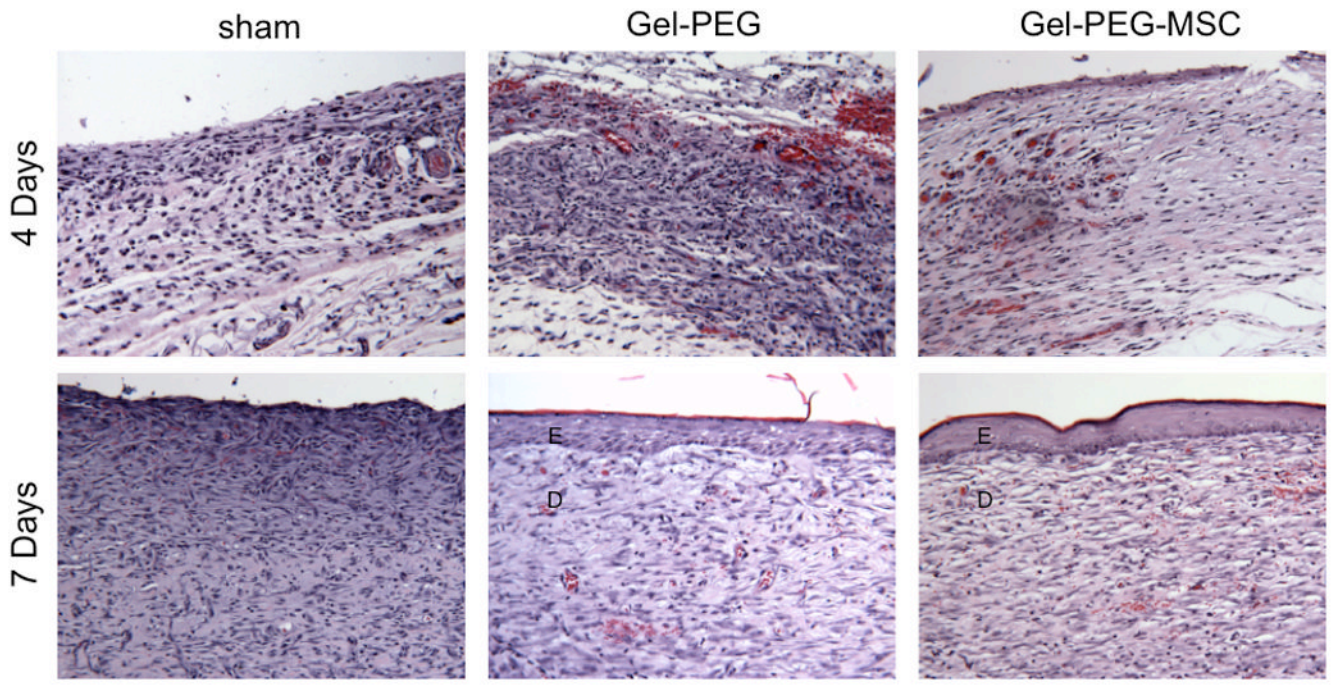

Figure 6.
H&E representative full-thickness wound images in the central area of the wound at 4 and 7 days (20x magnification). Sham = sham wound, Gel-PEG = Gelatin/poly(ethyleneglycol) hydrogel, Gel-PEG-MSC = Gelatin/poly(ethylene glycol) biomatrix, E = Epidermis (immature), D = dermis (remodeling).

NIH-PA Author Manuscript
NIH-PA Author Manuscript
NIH-PA Author Manuscript

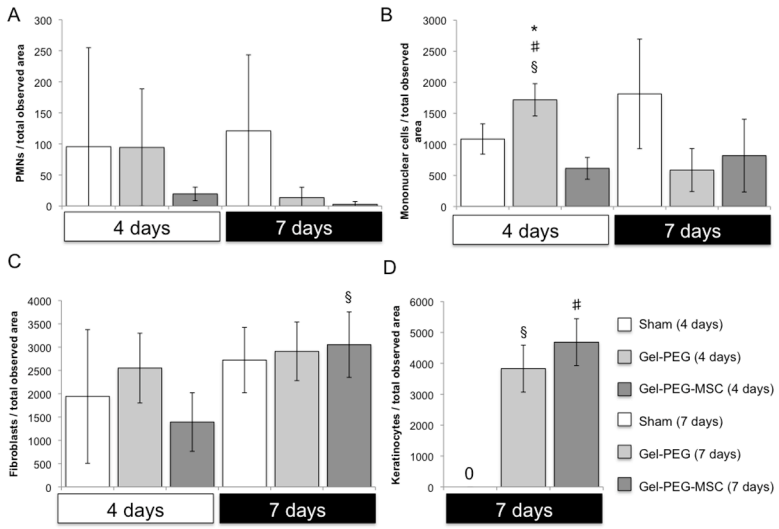

Figure 7.

Number of PMNs (A), mononuclear cells (B), fibroblasts (C), and keratinocytes (D) in each observed wound image area harvested from the central area of the wound (20x magnification) for each treatment group (n = 3) at 4 and 7 days. Sham = Sham wound, Gel-PEG = Gelatin/poly(ethylene glycol) hydrogel, MSC-gelatin/poly(ethylene glycol) biomatrix. Number of mononuclear cells per observed wound image area with the gelatin/poly(ethylene glycol) hydrogel treatment was statistically greater than the MSC-gelatin/poly(ethylene glycol) biomatrix treatment (#p = 0.0036) and the sham control (§p = 0.037) at 4 days. Number of mononuclear cells per observed wound image area with the gelatin/poly(ethylene glycol) hydrogel treatment at 4 days was statistically greater than (*p = 0.011) 7 days for the same treatment. Number of fibroblasts per observed wound image area with the MSC-gelatin/poly(ethylene glycol) hydrogel treatment at 7 days was statistically greater than (§p = 0.038) at 4 days for the same treatment. Number of keratinocytes per observed wound image area for the gelatin/poly(ethylene glycol) hydrogel treatment (§p = 0.00095) and the MSC-gelatin/poly(ethylene glycol) biomatrix (#p = 0.00043) was statistically greater than the sham control at 7 days.

NIH-PA Author Manuscript
NIH-PA Author Manuscript
NIH-PA Author Manuscript

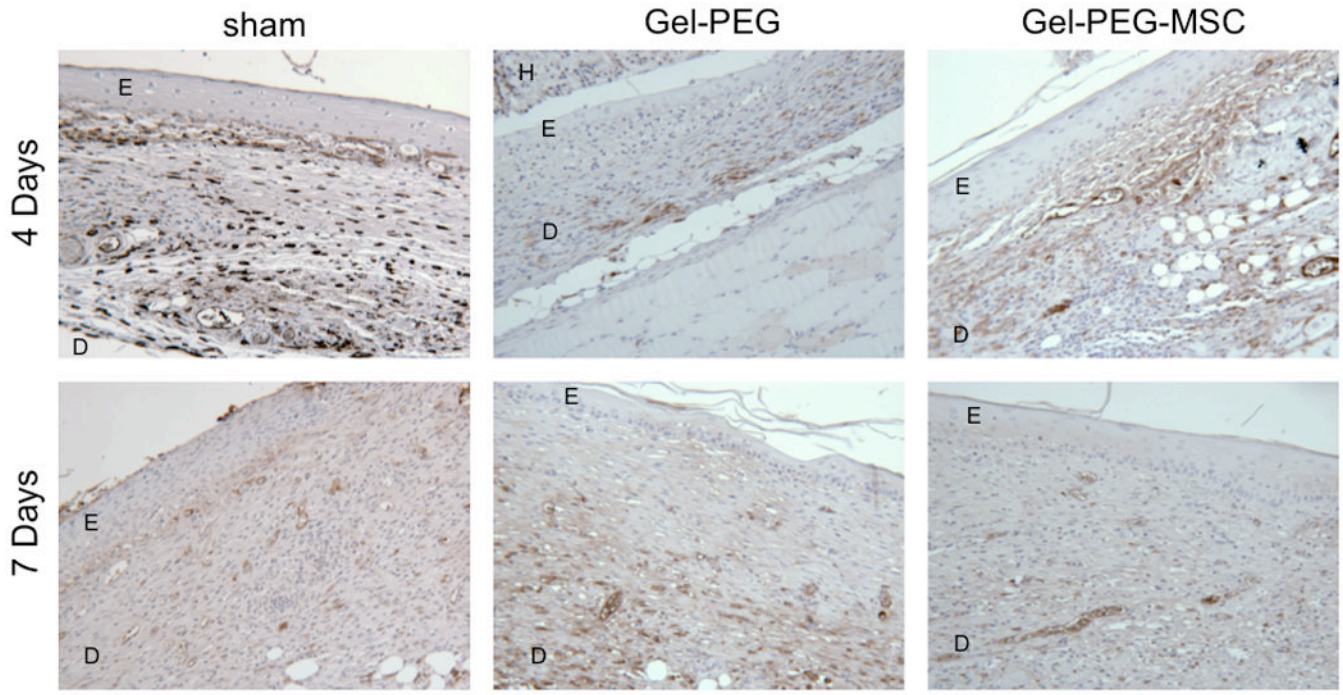

Figure 8.

Representative full-thickness wound images in the central area of the wound at 4 and 7 days (20x magnification). Macrophages were immunostained for CD163 (an anti-inflammatory macrophage marker) and the wound area was counterstained with hematoxylin. Sham = sham wound, Gel-PEG = Gelatin/poly(ethylene glycol) hydrogel, Gel-PEG-MSC = Gelatin/poly(ethylene glycol) biomatrix, E = Epidermis (immature), D = dermis (remodeling), H = Gelatin/poly(ethylene glycol) hydrogel.

NIH-PA Author Manuscript

NIH-PA Author Manuscript

NIH-PA Author Manuscript

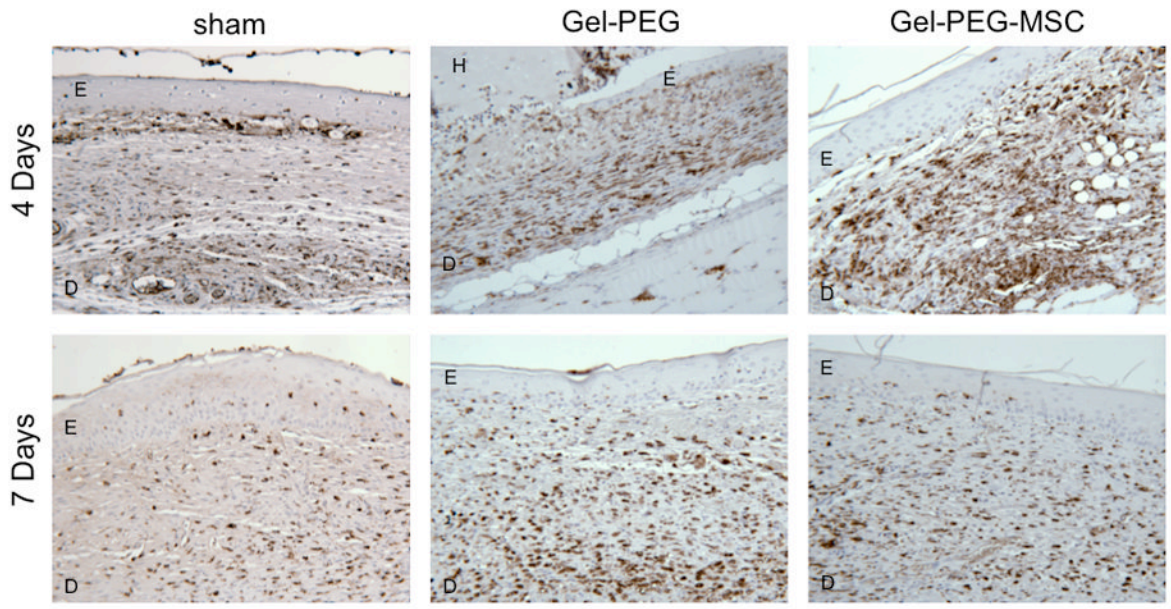

Figure 9.

Representative full-thickness wound images in the central area of the wound at 4 and 7 days (20x magnification). Macrophages were immunostained for CD68 (a pan-macrophage marker) and the wound area was counterstained with hematoxylin. Sham = sham wound, Gel-PEG = Gelatin/poly(ethylene glycol) hydrogel, Gel-PEG-MSC = Gelatin/poly(ethylene glycol) biomatrix, E = Epidermis (immature), D = dermis (remodeling), H = Gelatin/poly(ethylene glycol) hydrogel.

NIH-PA Author Manuscript
NIH-PA Author Manuscript
NIH-PA Author Manuscript

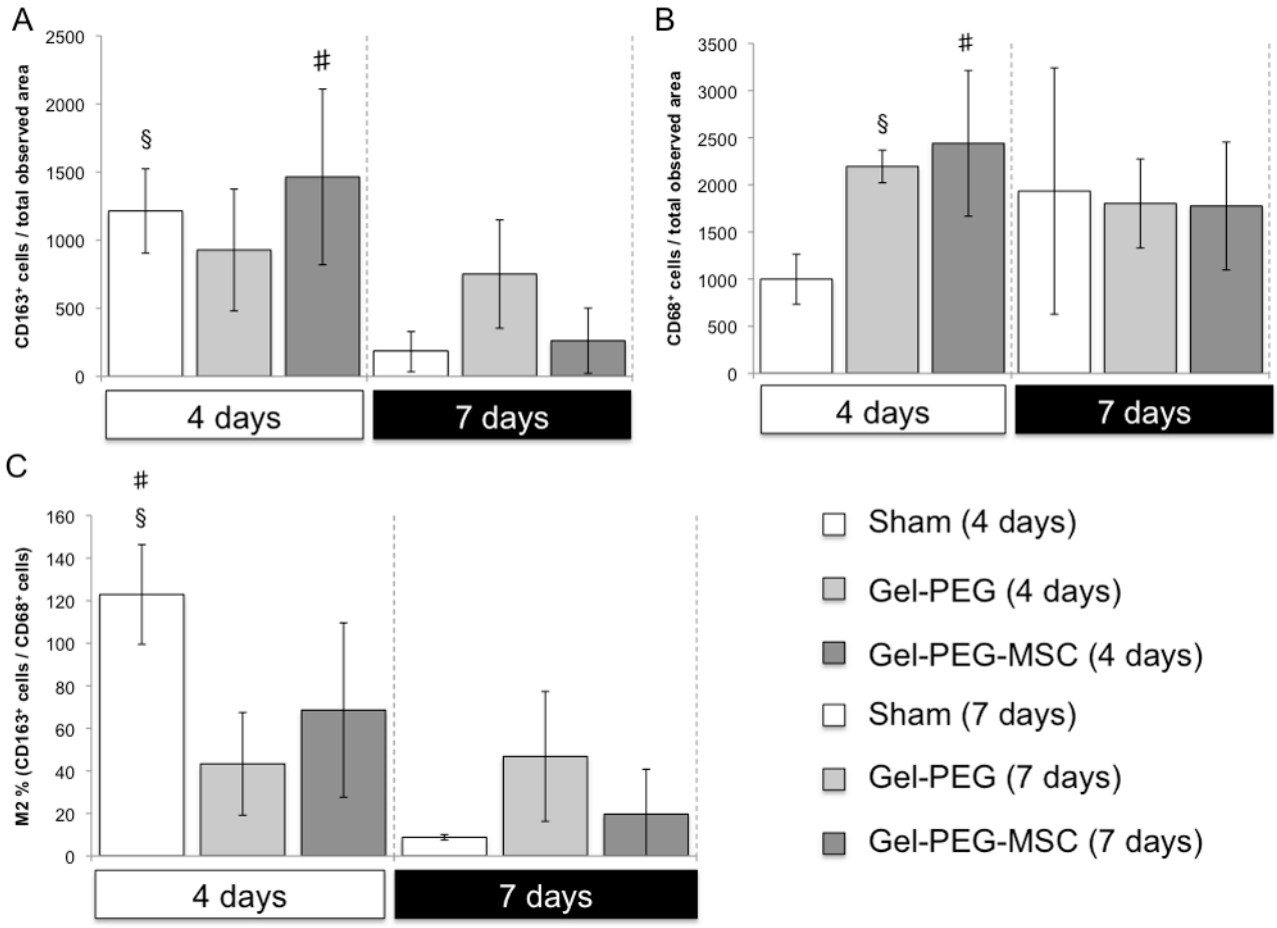

Figure 10.

Number of positive macrophages for specific cell surface markers in each observed wound image area harvested from an area adjacent to the central area of the wound (20x magnification) for each treatment group (n = 3) at 4 and 7 days and the macrophage M2 percentage ($CD163^+/CD68^+$). A: Number of $CD163^+$ cells (an anti-inflammatory macrophage marker) per observed wound area from image taken from an area adjacent to the central area of the wound (20x magnification) for each treatment group (n = 3) at 4 and 7 days. Sham = Sham wound, Gel-PEG = Gelatin/poly(ethylene glycol) hydrogel, Gel-PEG-MSC = MSC-gelatin/poly(ethylene glycol) biomatrix. Number of $CD163^+$ cells per observed wound image area was statistically greater ($p = 0.0064$) for the sham control at 4 days as compared to 7 days for the same treatment group and number of $CD163^+$ cells per observed wound image area was also statistically greater for the gelatin/poly(ethylene glycol) biomatrix at 4 days as compared to 7 days for the same treatment group (#p = 0.038). B: Number of $CD68^+$ cells (an pan-macrophage marker) per observed wound image area taken from an area adjacent to the central area of the wound (20x magnification) for each treatment group (n = 3) at 4 and 7 days. Number of $CD68^+$ cells per observed wound image area was statistically greater for the gelatin/poly(ethylene glycol) hydrogel treatment (§p = 0.0028) and gelatin/poly(ethylene glycol) biomatrix (#p = 0.037) than the sham control at 4 days. C: The M2 percentage ($CD163^+/CD68^+$) from the number of $CD163^+$ and $CD68^+$ cells from respective observed wound image areas (Figure 11 and Figure 12) at 4 and 7 days for each treatment group (n = 3). The M2 percentage ($CD163^+/CD68^+$) was statistically greater for the sham wound when compared to the gelatin/poly(ethylene glycol) treatment (§p =

NIH-PA Author Manuscript

NIH-PA Author Manuscript

NIH-PA Author Manuscript

0.014) at 4 days and was also statistically greater than the sham wound at 7 days (#p = 0.0011).

NIH-PA Author Manuscript
NIH-PA Author Manuscript
NIH-PA Author Manuscript

Table 1

Gelatln/poly(ethytene glycol) hydrogel formation parameters and rates of gelation means ± SD (n = 5).

	8% gel-PEG-SH	**10% gel-PEG-SH**	**12% gel-PEG-SH**
pH 7.5	no gelation	no gelation	> 1200 sec
pH 8.5	557 ± 25 sec	106 ± 8 sec	25 ± 3 sec
pH 9.5	85 ± 6 sec	29 ± 3 sec	14 ± 1 sec